IEEE Access
Multidisciplinary ⋮ Rapid Review ⋮ Open Access Journal

Received 29 November 2022, accepted 22 December 2022, date of publication 28 December 2022, date of current version 2 January 2023.

Digital Object Identifier 10.1109/ACCESS.2022.3232945

RESEARCH ARTICLE

Trajectory Optimization and Power Allocation for Cell-Free Satellite-UAV Internet of Things

ZHAO WU, (Member, IEEE), AND QIANG WANG
Guangxi Colleges and Universities Key Laboratory of Complex System Optimization and Big Data Processing, Yulin Normal University, Yulin 537000, China
Research Center for Intelligent Information and Communication Technology, Yulin Normal University, Yulin 537000, China

Corresponding author: Qiang Wang (wangqiangzhch@foxmail.com)

This work was supported in part by the Guangxi Natural Science Foundation under Grant 2021GXNSFBA196076; in part by the General Project of Guangxi Natural Science Foundation Project (Guangdong-Guangxi Joint Fund Project) under Grant 2021GXNSFAA075031; in part by the Basic Ability Improvement Project of Young and Middle-Aged Teachers in Guangxi Universities under Grant 2022KY0579; and in part by the Guangxi Key Laboratory of Precision Navigation Technology and Application, Guilin University of Electronic Technology, under Grant DH202007.

ABSTRACT Massive access outside the coverage of terrestrial cellular networks will be the main feature of the sixth generation (6G) networks. In order to cope with it, the cognitive satellite-UAV network (CSUN) has drawn a lot of attentions. In this paper, we investigate the UAV trajectory optimization and power allocation for the cell-free CSUN consisting of one satellite and a swarm of UAVs. Indeed, due to the on-board energy constraints of UAVs, both the trajectory optimization and the power allocation can significantly save the energy to improve the energy efficiency. The joint trajectory optimization and power allocation problem is formulated as a mixed-integer non-convex optimization problem which is extremely difficult to solve. In order to reduce the computational complexity, we decompose the original optimization problem into two subproblems in terms of the trajectory optimization and power allocation. For the trajectory optimization subproblem, we model it as a Traveling Salesman Problem (TSP), and the PSO is adopted to solve it. When the trajectory variables are fixed, the power allocation subproblem is still difficult to tackle due to its non-convexity and large scale. Firstly, we present a kind of centralized algorithm in which the DC (difference of two convex functions) algorithm is applied to optimize it, and then a distributed algorithm based on auxiliary variables is proposed to reduce the signaling overhead and computational complexity. The simulation results demonstrate the effectiveness of the proposed joint trajectory optimization and power allocation algorithm for the cell-free CSUN.

INDEX TERMS Cell-free, satellite-UAV network, power allocation, NOMA.

I. INTRODUCTION

The wide-area coverage with a massive number of devices, especially for the remote areas, such as the ocean, and the desert etc., has been identified as one of the main objectives of the upcoming sixth generation (6G) networks [1], [2], [3]. There are some challenges for the network construction in these remote areas. One challenge is that these areas are not suitable for large-scale construction of base stations due to the limitation of the geographical environments [4]. The other challenge is that the devices are always sparsely and unevenly distributed in wide areas which will cause unacceptable construction cost for the terrestrial cellular networks.

Under the above circumstances, the satellite network has become a promising solution to overcome these challenges due to the advantage of seamless coverage [5], [6]. Unfortunately, it is difficult to support massive access for the satellite network as a result of the limited transmission rate and large latency. Thus, the integration of the satellite network and unmanned aerial vehicles (UAVs) communication is regarded as an effective solution for the wide-area coverage with massive access [7], [8]. Indeed, flexible deployment and strong mobility are the advantages of the UAVs, which are suitable for the sparsely and unevenly distributed of the devices in wide areas. The tricky thing of the UAVs communication is

The associate editor coordinating the review of this manuscript and approving it for publication was Marco Martalo.

the limitation of the on-board energy, which will limit the flight time and the energy for the signal transmission. Therefore, the trajectory optimization for the UAVs is necessary which can significantly save the energy consumed for flight.

In order to improve the spectrum efficiency, the cognitive satellite-UAV network, in which UAV users and satellite users can share the same time-frequency resource, is considered by a lot of works [9], [10]. Since the distance from the satellite to ground is farther, the power control of the UAVs should be optimized carefully to reduce the interference to the satellite users. In addition, the cell-free network is also one of the enabling technologies of 6G, where a larger number of access points (APs) can simultaneously serve a smaller number of devices. Indeed, the cell free network can be regarded as a virtual distributed massive multiple-input multiple-output (MIMO) system which can effectively improve the coverage probability [11], [12], [13].

A. RELATED WORKS

In this subsection, we introduce the related works of the UAV assisted networks and satellite communication networks. UAV-assisted communication has been widely investigated since it can avoid obstacles and provide the line-of-sight (LoS) communication with ground devices due to the high mobility of UAVs. Therefore, the UAVs can be regarded as either base stations [14], [15], [16], [17], or mobile relays [18], [19], [20], [21], [22]. Reference [14] investigates the joint optimization of trajectory and resource allocation for the multi-UAV assisted backscatter communication network. In [14], the joint optimization of trajectory and resource allocation problem is formulated as a nonconvex optimization problem to maximize the max-min rate of the backscatter communication network. Particularly, the trajectory design in [14] is proposed to maximize system throughput. Reference [15] considers the UAV-enabled wireless sensor networks without eavesdropper's CSI. In [15], an adaptive secrecy transmission policy based on the Wyner encoding scheme is proposed, and then a secrecy energy efficiency (SEE) maximization problem is formulated to jointly optimize the resource allocation and UAV trajectory. Reference [16] evaluates the performance of the UAV integrated terrestrial cellular network (UTCN) using the tools of stochastic geometry. The results in [16] show that the performance of the UTCN will be degraded when the density of the UAVs is sufficiently large. Reference [17] investigates a dual UAV enabled secure communication system. In the scenario of [17], a UAV moves around to send confidential messages to a mobile user while another cooperative UAV transmits artificial noise signals to confuse malicious eavesdroppers. In [17], a a worst-case secrecy rate maximization problem is formulated, and it is tackled by optimizing the three-dimensional trajectory of UAVs and time allocation.

Reference [18] considers a UAV-assisted wireless sensor network where the UAVs paly a role of relays. In [18], the power control and trajectory planning for the UAV-assisted wireless sensors network are investigated to reduce the interference between the sensors and UAVs. Reference [21] proposes a kind of UAV-aided two way relay networks with users pair, where the UAV receives and buffers the signals from one user of the pair, and then forwards the signal to the other user when the UAV is close to the other. In [22], the authors propose an energy-constrained UAV-enabled mobile relay assisted secure communication system, and a joint optimization problem is formulated to enhance the reliability and security of the system.

Space-air-ground network is another promising technology for the wide-area Internet of Things (IoT) which is beneficial in terms of both providing the seamless coverage as well as of improving the capacity for users all over the world [23]. The cross-tier interference is a critical problem for the space-air-ground network if the spectrum sharing is adopted. Therefore, the trajectory design and the power allocation for the UAVs as well as satellite have been become the hot topics. Reference [24] investigates the joint UAV hovering altitude and power control problem for the space-air-ground IoT networks to reduce the cross-tier interference. Then, a two-stage joint resource allocation based on the Lagrange dual decomposition and concave-convex procedure method is proposed to solve the problem. Reference [25] investigates the joint resource allocation and UAV trajectory optimization for the space-air-ground IoT, in which the UAVs act as relays to upload the data from smart devices to low earth orbit satellites. Then, the joint optimization problem is formulated as a nonconvex optimization problem. The authors in [25] propose an iterative algorithm based on the variable substitution, successive convex optimization techniques, and the block coordinate decent algorithm to solve the nonconvex optimization problem. Reference [26] proposes a hybrid satellite-unmanned aerial vehicle relay network where the UAVs act as the relay from the satellite to the terrestrial users. In [26], the joint resource allocation in terms of the relay selection and power allocation is considered and then a metaheuristic teaching-learning based optimization algorithm is employed to optimize the problem. Mobile-edge caching is another hotspot which can effectively alleviate the heavy burden of backhaul. The space-air-ground integrated relay network is also considered in [27]. In [27], the UAV first amplifies the signals from the satellites through optimizing the detection vector. Then the UAV-ground NOMA communication is modeled as a energy efficiency optimization problem. The work in [28] considers a cache-enabled satellite-UAV-vehicle integrated network where the satellite acts as a cloud server, and the UAVs are regarded as the edge caching servers.

B. MOTIVATION AND CONTRIBUTIONS

As aforementioned, most of the prior works about the UAV trajectory design focus on the transmission rate maximization through optimizing the UAV trajectory. However, the energy consumed for flight is far more than the energy consumed for signal transmission. In addition, most of the related works about the satellite networks and UAV-assisted networks do not consider the distributed resource allocation algorithm which is crucial for the large-scale networks.

In this paper, we investigate the joint trajectory optimization and power allocation for the cell-free cognitive satellite-UAV IoT networks (CSUN). The objective of the trajectory optimization is to search the shortest route for the UAVs to save the on-board energy. For the power allocation, we present a kind of centralized algorithm where the DC (difference of two convex functions) algorithm is empolyed to optimize it, and then a distributed algorithm is proposed to reduce the signaling overhead and computational complexity.

The main contributions of this paper are summarized as follows:

1) We propose a kind of joint optimization framework for the trajectory optimization and power allocation of the cell-free CSUN. The joint trajectory optimization and power allocation is formulated as a mixed integer nonconvex programming problem (MINP). Particularly, the total distance traveled by the UAV swarm is integrated into the energy constraint of the MINP.
2) The formulated MINP is a large scale nonconvex optimization problem. In order to reduce the computational complexity, the original optimization problem is decomposed into two subproblems in terms of the trajectory optimization and power allocation. Specifically, the trajectory optimization problem is a combinatorial optimization problem, and we model it as a Traveling Salesman Problem (TSP). Then, a kind of PSO for TSP is adopted to optimize the trajectory optimization problem.
3) The power allocation subproblem is still extremely difficult to tackle due to the nature of nonconvexity. The DC (difference of two convex functions) method is used to solve the power allocation subproblem, and then we propose a distributed algorithm through introducing the auxiliary variables to reduce the signaling overhead and computational complexity.

The rest of the paper is organized as follows. Section II describes the system model for the cell-free CSUN. The UAV trajectory optimization is introduced in section III. In section IV, we optimize the power allocation problem using DC programming method, and a distributed algorithm is proposed in section V. In section VI, simulation results are provided to evaluate the performance of the proposed algorithm. Finally, we conclude this paper in section VII.

II. SYSTEM MODEL

In this paper, we consider a downlink of a wide-area IoT-oriented cell-free CSUN as shown in Fig.1, in which there are a satellite, K single-antenna UAVs, N_s single-antenna satellite users, and N_U single-antenna UAV users. To improve the spectrum efficiency, the satellite and all the UAVs share the same time-frequency resource. It is assumed that all the UAV users are divided into N groups according to the distances among the UAV users, and the n-th user group will be served in the n-th time slot. The number of the users in the n-th user group is denoted by U_n. The cell-free architecture is applied to improve the coverage probability, where all UAVs serve all the UAV users in the same user group. The hover-to-serve mode is considered, in which the UAV swarm transmit data when they are hovering above a group of users, and after the transmission, they will fly to the overhead of the next user group. The bandwidth is divided into G subcarriers, and each subcarrier can be assigned to at most one UAV user in each time slot in order to mitigate the intra-group interference. Since the subcarrier assignment problem has been investigated by a lot of works, we assume that the subcarrier assignment is fixed in this paper.

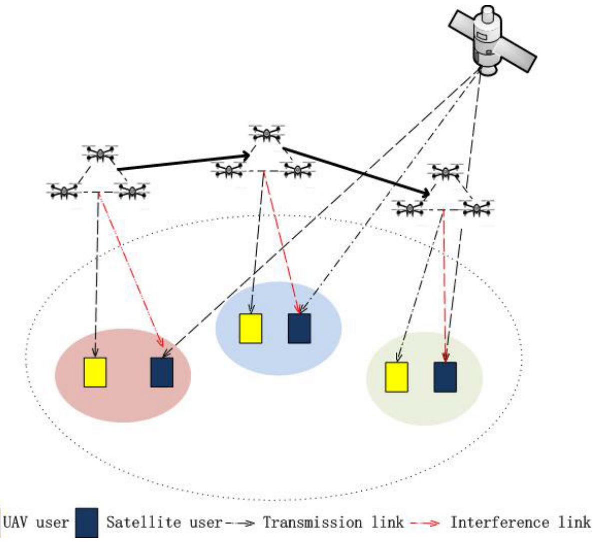

FIGURE 1. System model of the cell-free satellite-UAV network.

Due to the energy limitation of UAV, the trajectory optimization is considered to decrease the energy consumption for flight. For the sake of simplicity, we assume that the plane coordinate of the UAV swarm hovering above one certain user group is fixed, and the altitude of the UAV swarm is constant throughout the transmission process. The plane coordinate of the UAV swarm hovering above the n-th user group is denoted as (x_n, y_n). Let Z denote the total distance traveled by the UAV swarm, and Z can be expressed as:

$$Z = \sum_{i=1}^{N} \sum_{j=1}^{N} d_{ij} w_{ij} \tag{1}$$

where $d_{ij} = \sqrt{(x_i - x_j)^2 + (y_i - y_j)^2}$ denotes the distance between the i-th user group and the j-th user group; $w_{ij} \in \{0, 1\}$ indicates whether the path between the i-th user group and the j-th user group is chosen or not;

A. SIGNALS MODEL

Since the cell-free transmission mode is considered, all the UAVs serve all the users in the same user group simultaneously. The received signal of the u-th user in the n-th group on the g-th subcarrier can be given as:

$$r_{n,u,g} = \sum_{k=1}^{K} h_{n,u,g,k} s_{n,u,g,k} + z_{n,u,g} \tag{2}$$

where $h_{n,u,g,k}$ and $s_{n,u,g,k}$ are the channel coefficient and the transmit symbol from the k-th UAV to the u-th user in the n-th user group using the g-th subcarrier, respectively. $h_{n,u,g,k} = \beta_0 d_{n,u,k}^{-2}$, where β_0 is the channel gain at a reference distance of 1 meter(m), and $d_{n,u,k}$ is the distance between the k-th UAV and the u-th user in the n-th group. $z_{n,u,g} \sim \mathcal{CN}(0, \sigma^2)$ is the additive white Gaussian noise at the u-th user in the n-th user group using the g-th subcarrier.

In order to improve the spectrum efficiency, we assume that the satellite and UAVs share the same spectrum resources. In this paper, we only consider the leakage interference from the UAV to the satellite users and ignore the leakage interference from the satellite to the UAV users since it is relatively weak. The interference from the UAV swarm to the i-th satellite user in the n-th time slot is given by:

$$I_{n,i} = \sum_{u=1}^{U_n} \sum_{k=1}^{K} \sum_{g=1}^{G} h_{n,i,k} p_{n,u,g,k} \tag{3}$$

where $h_{n,i,k}$ denotes the channel coefficient from the k-th UAV to the i-th satellite user in the n-th time slot. $h_{n,i,k} = \beta_0 d_{n,i,k}^{-2}$, and $d_{n,i,k}$ represents the distance between the k-th UAV and the i-th satellite user in the n-th time slot. $p_{n,u,g,k}$ is the transmit power of the k-th UAV to the u-th user of the n-th user group.

In this paper, we consider the propulsion energy and communication energy for the UAVs, and the on-board energy constraints of UAVs is formulated as follows [?].

$$\frac{c}{\eta_k} \sum_{n=1}^{N} \sum_{u=1}^{U_n} \sum_{g=1}^{G} p_{n,u,g,k} T + p_k^{rc} T + E_k^{ind} + Z\xi \le E_k^{ob}, \forall k \tag{4}$$

where c is the power loss coefficient, η_k denotes the efficiency of power amplifiers in radio frequency chains. T is the total flight time of the UAV, and it dependents on the trajectory of the UAV. p_k^{rc} is the circuit power consumption of the k-th UAV. E_k^{ind} represents the energy consumed by the cooling system, which is transmit-power-independent. ξ is the energy consumption constant per unit distance.

Since both p_k^{rc} and E_k^{ind} are fixed for the given trajectories, we simplify the constraint 4 as

$$\frac{c}{\eta_k} \sum_{n=1}^{N} \sum_{u=1}^{U_n} \sum_{g=1}^{G} p_{n,u,g,k} T + Z\xi \le E_k, \forall k \tag{5}$$

where $E_k = E_k^{ob} - p_k^{rc} T - E_k^{ind}$.

It is assumed that the channels from the UAVs to the u-th user in the n-tn user group using the g-th subcarrier can be sorted as:

$$h_{n,u,g,1} \le h_{n,u,g,2} \le \cdots \le h_{n,u,g,K} \tag{6}$$

It can be regarded as a multiple APs and one user NOMA system, in which the signals with the better channel conditions have priority to be decoded, however, the signals with worse signals is still useful for the corresponding user, and they cannot be subtracted. Therefore, in the multiple APs and one user NOMA system, the signals with the better channel conditions will be interfered by the signals with the worse channel conditions. Thus, the transmit rate of the u-th user in the n-th user group using the g-th subcarrier can be written as:

$$R_{n,u,g} = \sum_{k=1}^{K} \log(1 + \frac{h_{n,u,g,k} p_{n,u,g,k}}{\sum_{l=1}^{k-1} h_{n,u,g,l} p_{n,u,g,l} + \sigma^2}) \tag{7}$$

B. PROBLEM FORMULATION

In this paper, we aim to optimize the trajectory of the UAV swarm and the power allocation to maximize the system throughput. The optimization problem can be formulated as follows:

$$\mathbf{P1} \ \max_{\mathbf{p},\mathbf{w}} \sum_{n=1}^{N} \sum_{u=1}^{U_n} \sum_{g=1}^{G} \sum_{k=1}^{K} \log(1 + \frac{h_{n,u,g,k} p_{n,u,g,k}}{\sum_{l=1}^{k-1} h_{n,u,g,l} p_{n,u,g,l} + \sigma^2}) \tag{8}$$

$$s.t. \sum_{u=1}^{U_n} \sum_{k=1}^{K} \sum_{g=1}^{G} h_{n,i,k} p_{n,u,g,k} \le I_{max}, \forall n, \forall i \tag{9}$$

$$\frac{c}{\eta_k} \sum_{n=1}^{N} \sum_{u=1}^{U_n} \sum_{g=1}^{G} p_{n,u,g,k} T + Z\xi \le E_k, \forall k \tag{10}$$

$$\sum_{u=1}^{U_n} \sum_{g=1}^{G} p_{n,u,g,k} \le P_{max}, \forall n, \forall k \tag{11}$$

$$p_{n,u,g,k} \ge 0, \forall n, u, g, k \tag{12}$$

where (9) is the interference constraint for the satellite users, and I_{max} means the the interference temperature threshold; (10) means the total energy constraint of the k-th UAV; (11) is the maximum transmit power constraint for each UAV.

Due to the combinatorial nature of the trajectory optimization, problem **P1** is a mixed integer nonlinear programming problem which is extremely difficult to tackle. In the following, to decrease the computational complexity, we first decompose **P1** into two subproblems in terms of the trajectory optimization and power allocation, respectively. Then, we model the trajectory optimization as a TSP, and adopt the PSO to optimize it. For the power allocation subproblem, we propose a central algorithm based on the DC programming method to solve it. Then, we propose a distributed algorithm through introducing the auxiliary variables in order to reduce the signaling overhead.

III. TRAJECTORY OPTIMIZATION

The trajectory optimization problem can be modeled as follows:

$$\textbf{P2}\ \min_{\mathbf{w}} Z = \sum_{i=1}^{N}\sum_{j=1}^{N} d_{ij}w_{ij} \tag{13}$$

$$s.t.\ \sum_{j=1}^{N} w_{ij} = 1, \forall i \in V \tag{14}$$

$$\sum_{i=1}^{N} w_{ij} = 1, \forall j \in V \tag{15}$$

$$\sum_{i\in S}\sum_{j\in S} w_{ij} \le |S| - 1, \forall S \in V, 2 \le |S| \le n-1 \tag{16}$$

$$w_{ij} \in \{0, 1\}, \forall i, \forall j \tag{17}$$

where Z and V are the total distance and the set of the user groups; S denotes a subset of V; constraints (14) and (15) are imposed to guarantee that each user group can be passed only once in each cycle; constraint (16) is imposed to guarantee that there is no sub loop solutions.

Problem **P2** is a TSP, which has been proved as a NP-hard problem, and the computational complexity will increase exponentially with the increase of the number of the user groups. In this paper, we adopt the PSO to optimize **P2** since the traditional deterministic algorithms are invalid. PSO is one of the swarm intelligence algorithms with fast converge speed, and it has a wide range of applications in science and industry [30].

In this paper, we adopt the PSO framework for solving TSP in [31]. The ith particle can be expressed as:

$$X_i = [x_{i1}, x_{i2}, \cdots, x_{iN}] \tag{18}$$

which means that the UAVs move following the path: $x_{i1} \longrightarrow x_{i2} \longrightarrow \cdots \longrightarrow x_{iN}$, and x_{in} is a integer from 1 to N, and it represents the n-th user group the UAVs passed.

Then, we introduce the evolutionary operator of the PSO for TSP. Firstly, the swap operator $SO(i1, i2)$ is defined, which means that the orders of x_{i1} and x_{i2} are switched. For example, if $X = [1, 2, 5, 3, 6, 4]$, and the swap operator is $SO(2, 6)$, then $X + SO(2, 6) = [1, 6, 5, 3, 2, 4]$. The ordered set of the swap operators is denoted by swap sequence, such as $S = (SO_1, \cdots, SO_k)$. The swap sequence acting on one solution represents that all the swap operators of the swap sequence act on the solution in order, which can be expressed as:

$$X + (SO_1, \cdots, SO_k) = ((X + SO_1) + SO_2) + \cdots + SO_k \tag{19}$$

Define $\oplus$ as the merging operator. For example, $X + (SO_1 \oplus SO_2)$ is equivalent to that SO_1 and SO_2 act on solution X in order.

Then, we introduce the difference between two solutions: $S = X_1 - X_2$, where S is a swap sequence, and it can be regarded as the velocity in PSO. Indeed, $S = X_1 - X_2$ is equivalent to $X_1 = X_2 + S$. For example, there are two solutions: $X_1 = [5, 1, 3, 2, 4, 6]$, and $X_2 = [2, 5, 1, 3, 6, 4]$. Since $X_1(1) = X_2(2)$, the first swap operator can be given as $SO_1(1, 2)$. We can obtain $X_2^1 = X_2 + SO_1 = [5, 2, 1, 3, 6, 4]$. Since $X_1(2) = X_2^1(3)$, the second swap operator is $SO_2(2, 3)$, and there is $X_2^2 = X_2^1 + SO_2(2, 3) = [5, 1, 2, 3, 6, 4]$. Repeating the above steps, we can obtain the third swap operator $SO_3(3, 4)$ and the fourth swap operator $SO_4(5, 6)$. Then, the difference between X_1 and X_2 can be expressed as $S = (SO_1, SO_2, SO_3, SO_4) = X_1 - X_2$. The multiplication of the real number and swap sequence cV is defined as that $[c]$ Vs are added, and then the first $[(c - [c])k]$ swap operators of V are added, where k is the number of the swap operators of V, and $[\cdot]$ represents the rounding operation.

The model of the PSO for TSP can be described as:

$$V_i' = V_i \oplus c_1r_1(P_i - X_i) \oplus c_2r_2(P_g - X_i) \tag{20}$$

$$X_i' = X_i + V_i' \tag{21}$$

where c_1, r_1, c_2, and r_2 are the learning coefficients. P_i is the best solution that this particle has reached, and P_g is the global best solution of all the particles. The PSO for trajectory optimization is shown in Algorithm 1, and Fig.2 shows the trajectory optimization results obtained by the exhaustive search, PSO, and random search, respectively.

As mentioned above, TSP is a combinatorial optimization problem. For the exhaustive search, if there are N groups, there are N choices in the first step, and $(N - 1)$ choices in the second step. Followed by analogy, the complexity of the exhaustive search is $\mathcal{O}(N!)$. In Algorithm 1, the computational complexity of the difference between two solutions is $\mathcal{O}(\frac{N(N+1)}{2})$, and the computational complexity of the swap operator is linear. Therefore, for each iteration of Algorithm 1, the computational complexity is $\mathcal{O}(\frac{N(N+1)}{2} + N)$. Assuming the total number of iterations is t, the total computational complexity of Algorithm 1 is $\mathcal{O}(t(\frac{N(N+1)}{2} + N))$, which is much lower than $\mathcal{O}(N!)$.

IV. POWER ALLOCATION OPTIMIZATION

In the above section, the trajectory optimization problem has been solved using the PSO. Then, there remain the power allocation variables in problem **P1**. Problem **P1** can be reformulated as:

$$\textbf{P3}\ \max_{\mathbf{p}} \sum_{n=1}^{N}\sum_{u=1}^{U_n}\sum_{g=1}^{G}\sum_{k=1}^{K} \log\Big(1 + \frac{h_{n,u,g,k}p_{n,u,g,k}}{\sum_{l=1}^{k-1} h_{n,u,g,l}p_{n,u,g,l} + \sigma^2}\Big) \tag{22}$$

$$s.t.\ \frac{c}{\eta_k}\sum_{n=1}^{N}\sum_{u=1}^{U_n}\sum_{g=1}^{G} p_{n,u,g,k} + Z^*\tau \le E_k, \forall k$$

$$(9), (11), (12) \tag{23}$$

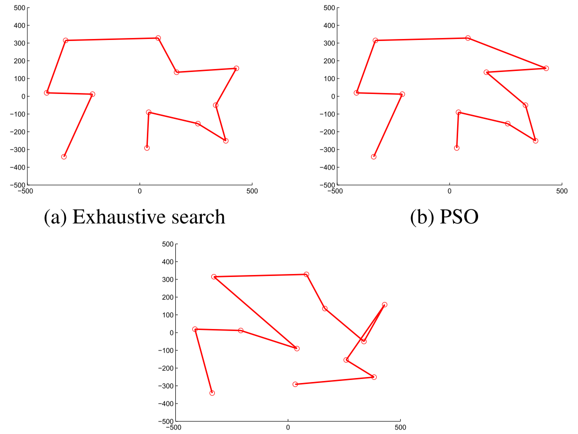

(a) Exhaustive search (b) PSO

(c) Random search

FIGURE 2. Optimized trajectory by the exhaustive search, PSO, and random search, respectively.

Algorithm 1 PSO for Trajectory Optimization

1: Initialization the particle swarm, and each particle is allocated an initial solution, and a random velocity, namely, a swap sequence;

2: For each particle X_i, computing its next position according to (20) and (21):
Computing $A = P_i - X_i$, and $B = P_g - X_i$, where both A and B are the swap sequences.
Computing the velocity V_i' according to (20), and the new position X_i' can be obtained in accordance with (21).
If X_i' is better than P_i, P_i is updated as X_i'.

3: If there is a new particle $\overline{X}$ is better than P_g, the global best solution P_g is updated as $\overline{X}$.

4: If the best global solution P_g meets the preset condition, output the global best solution.

The above optimization problem is still difficult to tackle since it is a nonconvex optimization problem. In this paper, we adopt the DC programming method [32] to optimize problem **P3**. Firstly, the objective function of **P3** can be rewritten as the difference of two convex functions as follows:

$$R = \sum_{n=1}^{N}\sum_{u=1}^{U_n}\sum_{g=1}^{G}\sum_{k=1}^{K}(\log(\sum_{l=1}^{k} h_{n,u,g,l}p_{n,u,g,l} + \sigma^2) \\ -\log(\sum_{l=1}^{k-1} h_{n,u,g,l}p_{n,u,g,l} + \sigma^2)) \quad (24)$$

We denote $H(\overline{\mathbf{p}}) = \log(\sum_{l=1}^{k-1} h_{n,u,g,l}p_{n,u,g,l} + \sigma^2)$, and then $H(\overline{\mathbf{p}})$ can be expanded by the first order Taylor expansion:

$$H(\overline{\mathbf{p}}) = H(\overline{\mathbf{p}}^{\nu}) + [\nabla H(\overline{\mathbf{p}}^{\nu})]^T(\overline{\mathbf{p}} - \overline{\mathbf{p}}^{\nu}) \quad (25)$$

where $\overline{\mathbf{p}} = [p_{n,u,g,1}, \cdots, p_{n,u,g,k-1}]$, and $\nabla H(\overline{\mathbf{p}}^{\nu})$ denotes the gradient of function H at the point $\overline{\mathbf{p}}$, and $[\cdot]^T$ means the transpose of the vector.

Then, substituting (25) into (24), (24) can be rewritten as:

$$R(\mathbf{p};\mathbf{p}^{\nu}) = \sum_{n=1}^{N}\sum_{u=1}^{U_n}\sum_{g=1}^{G}\sum_{k=1}^{K}(\log(\sum_{l=1}^{k} h_{n,u,g,l}p_{n,u,g,l} + \sigma^2) \\ -H(\overline{\mathbf{p}}^{\nu}) - [\nabla H(\overline{\mathbf{p}}^{\nu})]^T(\overline{\mathbf{p}} - \overline{\mathbf{p}}^{\nu})) \quad (26)$$

Obviously, (26) is a concave function.

Thus, problem **P3** can be rewritten as:

$$\textbf{P4} \max_{\mathbf{p}} \; R(\mathbf{p};\mathbf{p}^{\nu}) \\ s.t. \; (9), (11), (12), (23) \quad (27)$$

Problem **P4** is a convex optimization, since its objective is concave, and all of the constraints of **P4** are affine. Therefore, **P4** can be solved by the convex optimization technology.

We assume that $\widehat{\mathbf{p}}$ is the optimal solution of problem **P4**, and the iterative formula of $\mathbf{p}^{\nu}$ can be expressed as:

$$\mathbf{p}^{\nu+1} = \mathbf{p}^{\nu} + \beta(\widehat{\mathbf{p}} - \mathbf{p}^{\nu}) \quad (28)$$

where $\beta \in (0, 1)$. The details of the power allocation algorithm can be referred to the Algorithm 2.

Algorithm 2 The Power Allocation Optimization Using DC Programming

---

1: **Initialization**
2: set $\nu = 0$.
3: Initialize the power allocation variables $\mathbf{p}^0$.
4: **Updating**
5: **while** $\mathbf{p}^{\nu} - \mathbf{p}^{\nu-1} \succeq \tau_{thr}$ **do**
6: $\quad \nu = \nu + 1$;
7: $\quad$ Compute the optimal power allocation of **P3** $\hat{\mathbf{p}}$ using the convex optimization technology.
8: $\quad$ Updating power allocation $\mathbf{p}^{\nu}$ according to (28);
9: **end while**

V. DISTRIBUTED ALGORITHM

The algorithm in the above section is centralized which will consume a lot of signaling and computational overhead. Indeed, the objective of problem **P4** includes multiple nonadditive coupling variables which makes the problem difficult to be decomposed across the UAVs. In this section, we provide a distributed implementation of Algorithm 2.

In order to decouple the nonadditive variables. we introduce the auxiliary variables $\mathbf{t} = \{\mathbf{t}_{n,u,k}\}$, where $\mathbf{t}_{n,u,k} = \{t_{n,u,g,k}\}_{1\times G}$, and setting $0 < t_{n,u,g,k} \leq \sum_{l=1}^{k} h_{n,u,g,l}p_{n,u,g,l}$. Thus, problem **P4** cab be rewritten as:

$$\textbf{P5} \max_{\mathbf{t},\mathbf{p}} \; R(\mathbf{t},\mathbf{p};\mathbf{p}^{\nu}) \\ = \sum_{n=1}^{N}\sum_{u=1}^{U_n}\sum_{g=1}^{G}\sum_{k=1}^{K}(\log(t_{n,u,g,k} + \sigma^2) \\ -H(\overline{\mathbf{p}}^{\nu}) - [\nabla H(\overline{\mathbf{p}}^{\nu})]^T(\overline{\mathbf{p}} - \overline{\mathbf{p}}^{\nu})) \quad (29)$$

$$s.t.\ 0 < t_{n,u,g,k} \le \sum_{l=1}^{k} h_{n,u,g,l}p_{n,u,g,l}, \forall n, u, g, k$$
$$s.t.\ (9), (11), (12), (23) \tag{30}$$

It can be observed that problem **P5** and **P4** are equivalent. Indeed, in the case of $t_{n,u,g,k} = \sum_{l=1}^{k} h_{n,u,g,l}p_{n,u,g,l}$, problem **P5** is obviously equivalent to **P4**. If $t_{n,u,g,k} < \sum_{l=1}^{k} h_{n,u,g,l}p_{n,u,g,l}$, the maximum objective value of problem **P5** is less than that of problem **P4** due to the monotone increasing property of logarithmic function.

$\log(t_{n,u,g,k} + \sigma^2)$ is a ascending function with respect to variable $t_{n,u,g,k}$. Therefore, **P5** can be transformed as the epigraph form as follows:

$$\mathbf{P6}\ \max_{\mathbf{t},\ \mathbf{p}, R_{th}}\ R_{th} \tag{31}$$
$$s.t.\ R(\mathbf{t}, \mathbf{p}; \mathbf{p}^v) \ge R_{th}$$
$$s.t.\ (9), (11), (12), (23), (30) \tag{32}$$

Then, we introduce a feasible $S = \{\mathbf{p}^v, R_{th}^v, \mathbf{t}^v\}$, and any $\tau_{R_{th}}$, $\tau_{\mathbf{p}}$, and $\tau_{\mathbf{t}} > 0$. **P6** can be approximated as:

$$\mathbf{P7}\ \max_{\mathbf{t},\ \mathbf{p}, R_{th}}\ R_{th} - \frac{\tau_{R_{th}}}{2}(R_{th} - R_{th}^v)^2 - \frac{\tau_{\mathbf{p}}}{2}\|\mathbf{p}-\mathbf{p}^v\|_2^2 - \frac{\tau_{\mathbf{t}}}{2}\|\mathbf{t}-\mathbf{t}^v\|_2^2 \tag{33}$$
$$s.t.\ R(\mathbf{t}, \mathbf{p}; \mathbf{p}^v) \ge R_{th}$$
$$s.t.\ (9), (11), (12), (23), (30) \tag{34}$$

where the terms of $\frac{\tau_{R_{th}}}{2}(R_{th} - R_{th}^v)^2$, $\frac{\tau_{\mathbf{p}}}{2}\|\mathbf{p}-\mathbf{p}^v\|_2^2$, and $\frac{\tau_{\mathbf{t}}}{2}\|\mathbf{t}-\mathbf{t}^v\|_2^2$ are imposed to improve the convexity of the objective function.

Let $\mathbf{S} = (\mathbf{t}, \mathbf{p}, R_{th})$, and the Lagrangian function of problem **P7** can be written as:

$$\mathcal{L}(\mathbf{S}, \boldsymbol{\rho}, \boldsymbol{\theta}, \boldsymbol{\lambda}, \boldsymbol{\mu}; \mathbf{S}^v) = \mathcal{L}_{R_{th}}(R_{th}, \boldsymbol{\rho}; R_{th}^v) + \mathcal{L}_{\mathbf{p}}(\mathbf{p}, \boldsymbol{\rho}, \boldsymbol{\theta}, \boldsymbol{\lambda}, \boldsymbol{\mu}; \mathbf{p}^v) + \mathcal{L}_{\mathbf{t}}(\mathbf{t}, \boldsymbol{\rho}, \boldsymbol{\theta}; \mathbf{t}^v) \tag{35}$$

where $\boldsymbol{\lambda}$, $\boldsymbol{\eta}$, $\boldsymbol{\mu}$, $\boldsymbol{\theta}$ and ρ are the Lagrangian multipliers with respect to the constraints (9), (11), (23), (30), and (34). $\mathcal{L}_{R_{th}}(R_{th}, \boldsymbol{\rho}; R_{th}^v)$, $\mathcal{L}_{\mathbf{p}}(\mathbf{p}, \boldsymbol{\rho}, \boldsymbol{\theta}, \boldsymbol{\lambda}, \boldsymbol{\mu}; \mathbf{p}^v)$ and $\mathcal{L}_{\mathbf{t}}(\mathbf{t}, \boldsymbol{\rho}, \boldsymbol{\theta}; \mathbf{t}^v)$ are given in (36), (37), and (38), as shown at the bottom of the page, respectively.

Then, we can obtain the closed form solution of R_{th}, $\mathbf{p}$, and $\mathbf{t}$ as follows:

$$R_{th}^* = [\frac{1-\rho}{\tau_{R_{th}}} + R_{th}^v]^+ \tag{39}$$
$$t_{n,u,g,k}^* = [\frac{\Psi_{t_{n,u,g,k}}}{2\tau_{t_{n,u,g,k}}}]^+ \tag{40}$$
$$p_{n,u,g,k}^* = [\frac{\Psi_{p_{n,u,g,k}}}{\tau_{p_{n,u,g,k}}} + p_{n,u,g,k}^v]^+ \tag{41}$$

where

$$\Psi_{t_{n,u,g,k}} = -(\tau_{t_{n,u,g,k}}N_0 - \tau_{t_{n,u,g,k}}t^v + \theta) + \sqrt{(\tau_{t_{n,u,g,k}}N_0 - \tau_{t_{n,u,g,k}}t^v + \theta)^2 + 4\tau_{t_{n,u,g,k}}(\tau_{t_{n,u,g,k}}t^v + \rho - \theta N_0)},$$

and $\Psi_{p_{n,u,g,k}} = -(\lambda_{n,i}h_{n,i,k} + \mu_k + \eta_k + \rho\nabla_{p_{n,u,g,k}}H(\mathbf{p}_{n,u,g,k}^v))$. The details of the distributed dual algorithm can be referred to the Algorithm 3.

VI. SIMULATION RESULTS

In this section, we intend to evaluate the performance of the proposed joint trajectory design and power allocation scheme for the cell-free CSUN. In simulation, we assume that the sensor distribution area is a square with area of 1 Km $\times$ 1 Km, and there is one satellite in the considered cell-free CSUN. All the satellite users and UAV users are distributed in 12 regions. The number of the satellite users is set as 12, and each region includes one satellite user. The number of the UAV users is in the range from 60 to 300, and the flight altitude of the UAVs is set as 100 m. The the interference temperature threshold is set as -77dBm. The transmit power of the UAV is set as 30dBm, and the total energy carried by

$$\mathcal{L}_{R_{th}}(R_{th}, \boldsymbol{\rho}; R_{th}^v) = \frac{\tau_{R_{th}}}{2}(R_{th} - R_{th}^2)^2 - R_{th} + \rho R_{th} \tag{36}$$

$$\begin{aligned}\mathcal{L}_{\mathbf{p}}(\mathbf{p}, \boldsymbol{\lambda}, \boldsymbol{\mu}, \boldsymbol{\eta}, \boldsymbol{\theta}, \rho; \mathbf{p}^v) = \frac{\tau_{\mathbf{p}}}{2}\|\mathbf{p}-\mathbf{p}^v\|_2^2 &+ \sum_{n=1}^{N}\sum_{i=1}^{I}\lambda_{n,i}\sum_{u=1}^{U_n}\sum_{k=1}^{K}\sum_{g=1}^{G}h_{n,i,k}p_{n,u,g,k} - \sum_{n=1}^{N}\sum_{i=1}^{I}I_{max} + \sum_{k=1}^{K}\mu_k\sum_{n=1}^{N}\sum_{u=1}^{U_n}\sum_{g=1}^{G}p_{n,u,g,k} \\ &+ \sum_{k=1}^{K}\mu_k(Z^*\xi - E_k) + \sum_{n=1}^{N}\sum_{k=1}^{K}\eta_k\sum_{u=1}^{U_n}\sum_{g=1}^{G}p_{n,u,g,k} - \sum_{n=1}^{N}\sum_{u=1}^{U_n}\sum_{g=1}^{G}\sum_{k=1}^{K}\theta_{n,u,g,k}\sum_{l=1}^{k-1}h_{n,u,g,l}p_{n,u,g,l} \\ &- \sum_{n=1}^{N}\sum_{k=1}^{K}\eta_k P_{max} + \rho\sum_{n=1}^{N}\sum_{u=1}^{U_n}\sum_{g=1}^{G}\sum_{k=1}^{K}H(\mathbf{p}_{n,u,g,k}^v) + \rho\sum_{n=1}^{N}\sum_{u=1}^{U_n}\sum_{g=1}^{G}\sum_{k=1}^{K}[\nabla H(\mathbf{p}_{n,u,g,k}^v)^T](\mathbf{p}_{n,u,g,k} - \mathbf{p}_{n,u,g,k}^v)\end{aligned} \tag{37}$$

$$\mathcal{L}_{\mathbf{t}}(\mathbf{t}, \boldsymbol{\rho}, \boldsymbol{\theta}; \mathbf{t}^v) = \frac{\tau_{\mathbf{t}}}{2}\|\mathbf{t}-\mathbf{t}^v\|_2^2 - \rho\sum_{n=1}^{N}\sum_{u=1}^{U_n}\sum_{g=1}^{G}\sum_{k=1}^{K}\log(t_{n,u,g,k} + N_0) + \sum_{n=1}^{N}\sum_{u=1}^{U_n}\sum_{g=1}^{G}\sum_{k=1}^{K}\theta_{n,u,g,k}t_{n,u,g,k} \tag{38}$$

Algorithm 3 Distributed Dual Algorithm

Input $\boldsymbol{\lambda}^0 \succeq 0$, $\boldsymbol{\mu}^0 \succeq 0$, $\boldsymbol{\eta}^0 \succeq 0$, and $\boldsymbol{\theta}^0 \succeq 0$, and $\rho^0 \geq 0$; $\mathbf{S}^v = (\mathbf{p}^v, R^v_{th}, \mathbf{t}^v)$; Let $\boldsymbol{\Omega}^0 = (\boldsymbol{\lambda}^0, \boldsymbol{\mu}^0, \boldsymbol{\eta}^0, \boldsymbol{\theta}^0, \rho^0,)$; Set $\mathrm{v} = 0$.
Set the convergence threshold τ_{thr}.
Updating
while $\boldsymbol{\Omega}^v - \boldsymbol{\Omega}^{v-1} \succeq \tau_{thr}$ **do**
  $v = v + 1$;
  Compute the R^*_{th}, $\mathbf{p}^*$, and $\mathbf{t}^*$ according to (39)-(41).
  Update $\boldsymbol{\lambda}$, $\boldsymbol{\mu}$, $\boldsymbol{\eta}$, $\boldsymbol{\theta}$ and ρ according to subgradient method:

$$\lambda^{v+1}_{n,i} = \lambda^v_{n,i} + l^v(I_{max} - \sum_{n=1}^{U_n}\sum_{k=1}^{K}\sum_{g=1}^{G} h_{n,i,k}p^*_{n,u,g,k})$$

$$\mu^{v+1}_k = \mu^v_k + l^j((E_k - Z^*\xi) - \sum_{n=1}^{N}\sum_{u=1}^{U_n}\sum_{g=1}^{G} p^*_{n,u,g,k})$$

$$\eta^{v+1}_k = \eta^{v+1}_k + l^v(P_{max} - \sum_{u=1}^{U_n}\sum_{g=1}^{G} p^*_{n,u,g,k})$$

$$\theta^{v+1}_{n,u,g,k} = \theta^v_{n,u,g,k} + l^v(\sum_{l=1}^{k} h_{n,u,g,l}p^*_{n,u,g,l} - t^*_{n,u,g,k})$$

$$\rho^{v+1} = \rho^v + l^v(R(\mathbf{t}^*, \mathbf{p}^*; \mathbf{p}^v) - R^*_{th})$$

end while
output $\mathbf{S}^* = \mathbf{S}^{v+1}$

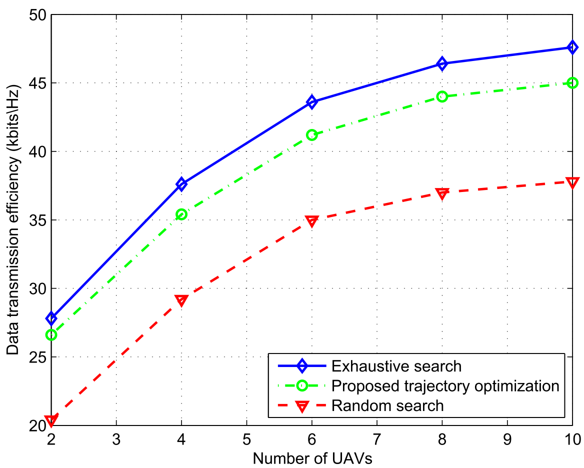

FIGURE 3. Sum rate for the exhaustive search, proposed trajectory optimization algorithm and random search with the increase of the number of UAVs.

the UAV battery is 2.7×10^4 J. The energy consumed for flight is set as 9 J per meter.

Fig.3 and Fig.4 evaluate the performance of the proposed trajectory optimization scheme using the PSO, and we compare the the performance of the proposed trajectory optimization scheme with that of the exhaustive search and random search. From Fig.3, it can be observed that the system throughput increases with the increase of the number of UAVs, and the slope of the curve becomes smaller with the increase of the number of UAVs. Furthermore, we can observe that the performance of the proposed trajectory optimization scheme using the PSO is slightly worse than that

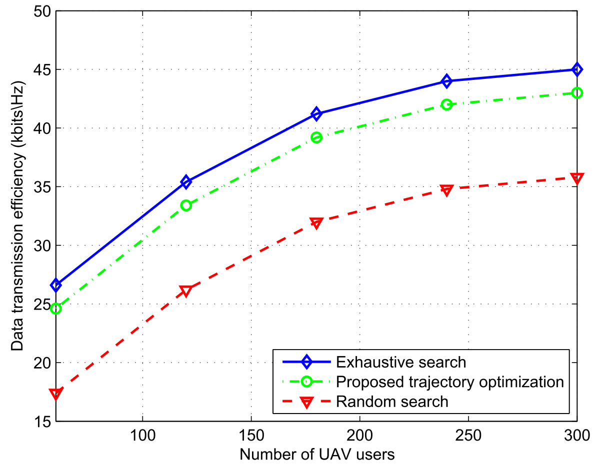

FIGURE 4. Sum rate for the exhaustive search, proposed trajectory optimization algorithm and random search with the increase of the number of UAVs.

of the exhaustive search. This result can be explained that the UAVs have to use more energy for flight for the trajectory obtained by the PSO, and the energy for the signal transmission is limited. In addition, we can also observe that the performance of the proposed trajectory optimization scheme outperforms that of the random search significantly. Indeed, the total distances of the trajectory obtained by the random search is too large, and the UAVs can not serve all the user groups in this case due to the limited on-board energy.

Fig.4 depicts the performance of the proposed trajectory optimization scheme with the increase of the number of UAV users. It can be observed from Fig.4 that the performance of the proposed trajectory optimization scheme increases with the increase of the number of UAV users, and this result can be explained by the multi-user diversity gain. Similarly with Fig.3, the performance of the proposed trajectory optimization scheme outperforms the random search, and the exhausted search has better performance than the proposed trajectory optimization scheme.

In the following, we evaluate the performance of the proposed joint trajectory optimization and power allocation scheme. Firstly, we introduce some benchmarks as follows.

1) Random trajectory optimization (RTO): In this benchmark, we adopt the random trajectory optimization, and the power allocation uses the proposed power allocation algorithm.
2) No power allocation (NPA): In this benchmark, the power allocation is fixed, and the proposed trajectory optimization scheme is adopted.
3) Random trajectory optimization and no power allocation (RTO & NPA): In this benchmark, the random trajectory optimization is adopted, and the power allocation is fixed.
4) Cell-free architecture with OMA access (CF-OMA): In this benchmark, the cell-free network and OMA

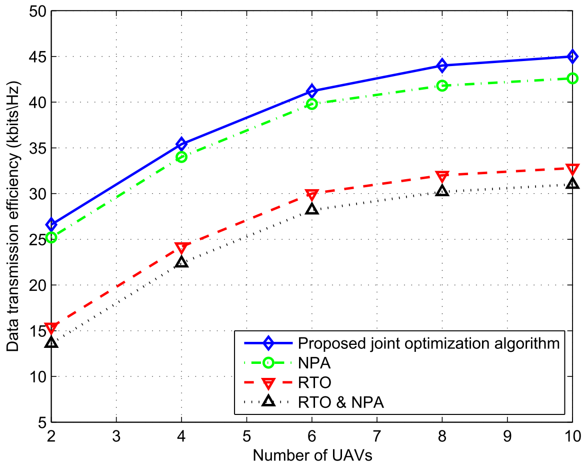

FIGURE 5. Sum rate for the exhaustive search, proposed trajectory optimization algorithm and random search with the increase of the number of UAVs.

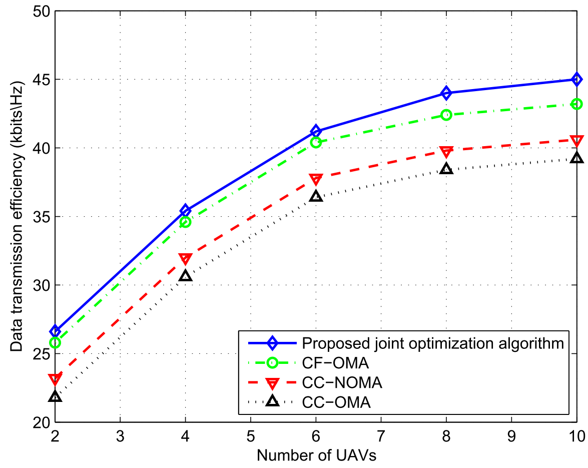

FIGURE 7. Sum rate for the exhaustive search, proposed trajectory optimization algorithm and random search with the increase of the number of UAVs.

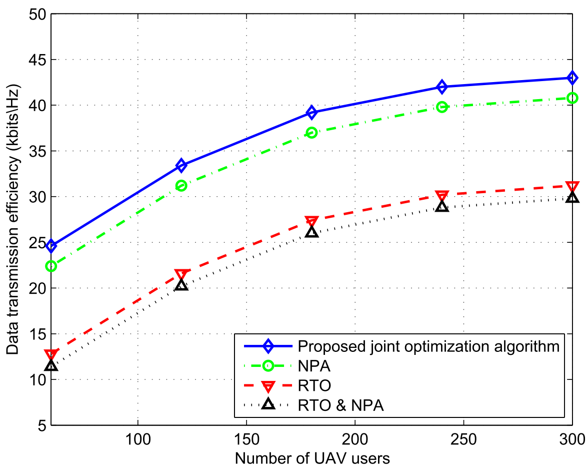

FIGURE 6. Sum rate for the exhaustive search, proposed trajectory optimization algorithm and random search with the increase of the number of UAVs.

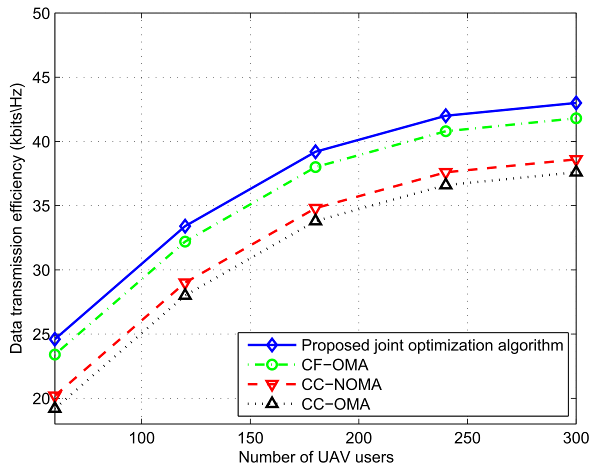

FIGURE 8. Sum rate for the exhaustive search, proposed trajectory optimization algorithm and random search with the increase of the number of UAVs.

are used as the network architecture and the multiple access, respectively.

5) Cell-centric architecture with NOMA access (CC-NOMA): In this benchmark, the cell-centric network is adopted, and the NOMA access is used as the multiple access.
6) Cell-centric architecture with OMA access (CC-OMA): In this benchmark, the cell-centric network is adopted, and the OMA access is used as the multiple access.

In Fig.5 and Fig.6, we compare the performance of the proposed joint trajectory optimization and power allocation scheme with that of the RTO benchmark, NPA benchmark, and RTO & NPA benchmark. From Fig.5, the performances of the proposed joint trajectory optimization and power allocation scheme and these benchmarks increase with the increase of the size of UAVs swarm, and the proposed joint trajectory optimization and power allocation scheme outperforms all these three benchmarks. This result illustrates the effectiveness of the proposed joint trajectory optimization and power allocation scheme. In addition, it can also be observed that the NPA benchmark has better performance than that of the RTO benchmark and RTO & NPA benchmark. This result shows that the trajectory optimization is more important than power allocation. Indeed, for the UAVs, the energy consumed for flight is the main part, and it is far more than the energy consumed for the signal transmission. The trajectory optimization can save more energy consumed for flight for the UAVs to transmit signals. Fig.6 shows the similar results with Fig.5, and it demonstrates the effectiveness of the proposed joint trajectory optimization and power allocation scheme. Fig.6 also depicts that the data transmission efficiency of the cell-free CSUN increases with the increase of the number of UAV users due to the multi-user diversity.

Next, we concentrate on analyzing the effectiveness of the user-centric networks and NOMA in Fig.7 and Fig.8. We compare the performance of the proposed joint trajectory optimization and power allocation scheme with that of the CF-OMA, CC-NOMA and CC-OMA. As shown by the curves, the data transmission efficiency of the network is improved with the increase of both the size of UAVs swarm and the number of UAV users due to the diversity gain. It can be seen from Fig.7 and Fig.8 that a better performance is achieved by the proposed joint trajectory optimization and power allocation scheme, and this phenomenon indicates the effectiveness of the cell-free networks and NOMA.

VII. CONCLUSION

In this paper, we consider a kind of cell-free CSUN to achieve the massive access and wide-area coverage for the IoT. The trajectory optimization and power allocation for the UAVs have been investigated to reduce the energy consumption and maximize the system throughput. The joint trajectory optimization and power allocation for the cell-free CSUN is formulated as MINP with high computational complexity, where the interference constraint for the satellite users is considered. In order to reduce the computational complexity, the original optimization problem is decomposed into two subproblems in terms of the trajectory optimization and power allocation. We formulate the trajectory optimization as a TSP, and the PSO is adopted to solve it. The power allocation subproblem is still difficult even through the trajectory optimization has been tackled due to the nonconvexity and large-scale of the problem. Firstly, we propose a centralized algorithm using the DC method, and then a distributed algorithm is proposed to reduce the signaling overhead.

REFERENCES

[1] S. Lee, J. Lee, H.-S. Park, and J. K. Choi, "A novel fair and scalable relay control scheme for Internet of Things in LoRa-based low-power wide-area networks," *IEEE Internet Things J.*, vol. 8, no. 7, pp. 5985–6001, Apr. 2021.

[2] X. Jiang, H. Zhang, E. A. B. Yi, N. Raghunathan, C. Mousoulis, S. Chaterji, D. Peroulis, A. Shakouri, and S. Bagchi, "Hybrid low-power wide-area mesh network for IoT applications," *IEEE Internet Things J.*, vol. 8, no. 2, pp. 901–915, Jan. 2021.

[3] M. Rahman and A. Saifullah, "Integrating low-power wide-area networks for enhanced scalability and extended coverage," *IEEE/ACM Trans. Netw.*, vol. 28, no. 1, pp. 413–426, Feb. 2020.

[4] X. Li, W. Feng, J. Wang, Y. Chen, N. Ge, and C.-X. Wang, "Enabling 5G on the ocean: A hybrid satellite-UAV-terrestrial network solution," *IEEE Wireless Commun.*, vol. 27, no. 6, pp. 116–121, Sep. 2020.

[5] Z. Jia, M. Sheng, J. Li, D. Niyato, and Z. Han, "LEO-satellite-assisted UAV: Joint trajectory and data collection for Internet of Remote Things in 6G aerial access networks," *IEEE Internet Things J.*, vol. 8, no. 12, pp. 9814–9826, Jun. 2020.

[6] M. Hua, Y. Wang, M. Lin, C. Li, Y. Huang, and L. Yang, "Joint CoMP transmission for UAV-aided cognitive satellite terrestrial networks," *IEEE Access*, vol. 7, pp. 14959–14968, 2019.

[7] J. Yu, X. Liu, Y. Gao, and X. Shen, "3D channel tracking for UAV-satellite communications in space-air-ground integrated networks," *IEEE J. Sel. Areas Commun.*, vol. 38, no. 12, pp. 2810–2823, Dec. 2020.

[8] Y. Zhu, W. Bai, M. Sheng, J. Li, D. Zhou, and Z. Han, "Joint UAV access and GEO satellite backhaul in IoRT networks: Performance analysis and optimization," *IEEE Internet Things J.*, vol. 8, no. 9, pp. 7126–7139, May 2021.

[9] C. Lei, W. Feng, Y. Chen, and N. Ge, "Joint power and channel allocation for safeguarding cognitive satellite-UAV networks," in *Proc. IEEE Global Commun. Conf. (GLOBECOM)*, Dec. 2021, pp. 1–6.

[10] X. Fang, Y. Wang, W. Feng, Y. Chen, and B. Ai, "Power allocation for maritime cognitive satellite-UAV-terrestrial networks," in *Proc. IEEE 19th Int. Conf. Cognit. Informat. Cognit. Comput. (ICCI*CC)*, Sep. 2020, pp. 139–143.

[11] S. Kusaladharma, W.-P. Zhu, W. Ajib, and G. A. A. Baduge, "Stochastic geometry based performance characterization of SWIPT in cell-free massive MIMO," *IEEE Trans. Veh. Technol.*, vol. 69, no. 11, pp. 13357–13370, Nov. 2020.

[12] A. Papazafeiropoulos, P. Kourtessis, M. D. Renzo, S. Chatzinotas, and J. M. Senior, "Performance analysis of cell-free massive MIMO systems: A stochastic geometry approach," *IEEE Trans. Veh. Technol.*, vol. 69, no. 4, pp. 3523–3537, Apr. 2020.

[13] H. Q. Ngo, A. Ashikhmin, H. Yang, E. G. Larsson, and T. L. Marzetta, "Cell-free massive MIMO versus small cells," *IEEE Trans. Wireless Commun.*, vol. 16, no. 3, pp. 1834–1850, Mar. 2017.

[14] Y. Du, Z. Chen, J. Hao, and Y. Guo, "Joint optimization of trajectory and communication in multi-UAV assisted backscatter communication networks," *IEEE Access*, vol. 10, pp. 40861–40871, 2022.

[15] M. Li, X. Tao, N. Li, H. Wu, and J. Xu, "Secrecy energy efficiency maximization in UAV-enabled wireless sensor networks without eavesdropper's CSI," *IEEE Internet Things J.*, vol. 9, no. 5, pp. 3346–3358, Mar. 2022.

[16] J. Liu, M. Sheng, R. Lyu, and J. Li, "Performance analysis and optimization of UAV integrated terrestrial cellular network," *IEEE Internet Things J.*, vol. 6, no. 2, pp. 1841–1855, Apr. 2019.

[17] W. Wang, X. Li, R. Wang, K. Cumanan, W. Feng, Z. Ding, and O. A. Dobre, "Robust 3D-trajectory and time switching optimization for dual-UAV-enabled secure communications," *IEEE J. Sel. Areas Commun.*, vol. 39, no. 11, pp. 3334–3347, Nov. 2021.

[18] S. Zhang, S. Shi, S. Gu, and X. Gu, "Power control and trajectory planning based interference management for UAV-assisted wireless sensor networks," *IEEE Access*, vol. 8, pp. 3453–3464, 2020.

[19] Z. Wang, F. Zhou, Y. Wang, and Q. Wu, "Joint 3D trajectory and resource optimization for a UAV relay-assisted cognitive radio network," *China Commun.*, vol. 18, no. 6, pp. 184–200, Jun. 2021.

[20] G. Zhang, X. Ou, M. Cui, Q. Wu, S. Ma, and W. Chen, "Cooperative UAV enabled relaying systems: Joint trajectory and transmit power optimization," *IEEE Trans. Green Commun. Netw.*, vol. 6, no. 1, pp. 543–557, Mar. 2022.

[21] Y. Liang, L. Xiao, D. Yang, Y. Liu, and T. Zhang, "Joint trajectory and resource optimization for UAV-aided two-way relay networks," *IEEE Trans. Veh. Technol.*, vol. 71, no. 1, pp. 639–652, Jan. 2022.

[22] W. Wang, X. Li, M. Zhang, K. Cumanan, D. W. K. Ng, G. Zhang, J. Tang, and O. A. Dobre, "Energy-constrained UAV-assisted secure communications with position optimization and cooperative jamming," *IEEE Trans. Commun.*, vol. 68, no. 7, pp. 4476–4489, Jul. 2020.

[23] F. Tang, L. Chen, X. Li, L. T. Yang, and L. Fu, "Intelligent spectrum assignment based on dynamical cooperation for 5G-satellite integrated networks," *IEEE Trans. Cognit. Commun. Netw.*, vol. 6, no. 2, pp. 523–533, Jun. 2020.

[24] J. Wang, C. Jiang, Z. Wei, C. Pan, H. Zhang, and Y. Ren, "Joint UAV hovering altitude and power control for space-air-ground IoT networks," *IEEE Internet Things J.*, vol. 6, no. 2, pp. 1741–1753, Apr. 2019.

[25] Y. Wang, Z. Li, Y. Chen, M. Liu, X. Lyu, X. Hou, and J. Wang, "Joint resource allocation and UAV trajectory optimization for space–air–ground Internet of Remote Things networks," *IEEE Syst. J.*, vol. 15, no. 4, pp. 4745–4755, Dec. 2021.

[26] S. Mirbolouk, M. Valizadeh, M. C. Amirani, and S. Ali, "Relay selection and power allocation for energy efficiency maximization in hybrid satellite-UAV networks with CoMP-NOMA transmission," *IEEE Trans. Veh. Technol.*, vol. 71, no. 5, pp. 5087–5100, May 2022.

[27] N. Wang, F. Li, D. Chen, L. Liu, and Z. Bao, "NOMA-based energy-efficiency optimization for UAV enabled space-air-ground integrated relay networks," *IEEE Trans. Veh. Technol.*, vol. 71, no. 4, pp. 4129–4141, Apr. 2022.

[28] S. Gu, X. Sun, Z. Yang, T. Huang, W. Xiang, and K. Yu, "Energy-aware coded caching strategy design with resource optimization for satellite-UAV-vehicle-integrated networks," *IEEE Internet Things J.*, vol. 9, no. 8, pp. 5799–5811, Apr. 2022.

[29] C. Liu, W. Feng, J. Wang, Y. Chen, and N. Ge, "Aerial small cells using coordinated multiple UAVs: An energy efficiency optimization perspective," *IEEE Access*, vol. 7, pp. 122838–122848, 2019.

[30] M. Zouari, N. Baklouti, J. Sanchez-Medina, H. M. Kammoun, M. B. Ayed, and A. M. Alimi, "PSO-based adaptive hierarchical interval type-2 fuzzy knowledge representation system (PSO-AHIT2FKRS) for travel route guidance," *IEEE Trans. Intell. Transp. Syst.*, vol. 23, no. 2, pp. 804–818, Feb. 2022.

[31] K.-P. Wang, L. Huang, C.-G. Zhou, and W. Pang, "Particle swarm optimization for traveling salesman problem," in *Proc. Int. Conf. Mach. Learn. Cybern.*, 2003, pp. 1583–1585.

[32] H. A. L. Thi, V. N. Huynh, and P. D. Tao, "DC programming and DCA for general DC programs," *Advanced Computational Methods for Knowledge Engineering*, vol. 282. 2014, pp. 15–35.

ZHAO WU (Member, IEEE) was born in Guangxi, China, in 1987. He received the B.E. degree in electronic and information engineering and the Ph.D. degree in electromagnetic fields and microwave technology from Xidian University, Xi'an, China, in 2011 and 2016, respectively. From October 2016 to March 2017, he was with Huawei Technologies Company Ltd. Since April 2017, he has been working as a Lecturer with the School of Physics and Telecommunication Engineering, Yulin Normal University. His research interests include metamaterials, novel antennas, and reconfigurable antenna design and applications.

QIANG WANG received the B.S. degree from Qufu Normal University, China, in 2010, and the M.Sc. and Ph.D. degrees from the Guangdong University of Technology, China. He is currently working with the Guangxi Colleges and Universities Key Laboratory of Complex System Optimization and Big Data Processing, Yulin Normal University, Yulin, China. His research interests include wireless communications, signal processing, and evolutionary algorithm.